Handbook of Clinical Neurology, Vol. 179 (3rd series)
The Human Hypothalamus: Anterior Region
D.F. Swaab, F. Kreier, P.J. Lucassen, A. Salehi, and R.M. Buijs, Editors
https://doi.org/10.1016/B978-0-12-819975-6.00008-X

Chapter 10

Spatial topography of the basal forebrain cholinergic projections: Organization and vulnerability to degeneration

TAYLOR W. SCHMITZ[1]* AND LASZLO ZABORSZKY[2]*

[1]*Department of Physiology and Pharmacology, University of Western Ontario, London, ON, Canada*
[2]*Center for Molecular and Behavioral Neuroscience, Rutgers University, Newark, NJ, United States*

Abstract

The basal forebrain (BF) cholinergic system constitutes a heterogeneous cluster of large projection neurons that innervate the entire cortical mantle and amygdala. Cholinergic neuromodulation plays a critical role in regulating cognition and behavior, as well as maintenance of cellular homeostasis. Decades of postmortem histology research have demonstrated that the BF cholinergic neurons are selectively vulnerable to aging and age-related neuropathology in degenerative diseases such as Alzheimer's and Parkinson's diseases. Emerging evidence from in vivo neuroimaging research, which permits longitudinal tracking of at-risk individuals, indicates that cholinergic neurodegeneration might play an earlier and more pivotal role in these diseases than was previously appreciated. Despite these advances, our understanding of the organization and functions of the BF cholinergic system mostly derives from nonhuman animal research. In this chapter, we begin with a review of the topographical organization of the BF cholinergic system in rodent and nonhuman primate models. We then discuss basic and clinical neuroscience research in humans, which has started to translate and extend the nonhuman animal research using novel noninvasive neuroimaging techniques. We focus on converging evidence indicating that the selective vulnerability of cholinergic neurons in Alzheimer's and Parkinson's diseases is expressed along a rostral-caudal topography in the BF. We close with a discussion of why this topography of vulnerability in the BF may occur and why it is relevant to the clinician.

INTRODUCTION

Basic and clinical neuroscience research on the basal forebrain (BF) cholinergic system has experienced somewhat of a renaissance in the past 15 years. Driven by advances in cell labeling techniques, electrophysiology and neuroimaging, our understanding of the organization and function of the BF cholinergic system and its primary neurochemical, acetylcholine, is coming into sharper focus. While acetylcholine was previously thought to operate in a single mode of regulating general states of alertness, characterized by global neuromodulation of cortical excitability, nonhuman animal research has demonstrated that this neurochemical is capable of modulating cortical activity at multiple spatial and temporal scales. In addition to the global excitation mode, acetylcholine can also excite or inhibit local cortical ensembles in time scales associated with specific cognitive and behavioral events, a mode which resembles wired neurotransmission (Sarter et al., 2009; Picciotto et al., 2012; Muñoz and Rudy, 2014; Ballinger et al., 2016; Obermayer et al., 2017; Schmitz and Duncan, 2018;

*Correspondence to: Taylor W. Schmitz, Ph.D., Department of Physiology and Pharmacology, University of Western Ontario, Perth Drive, London, ON, Canada N6A 3K7. Tel: +1-519-661-2111x80129, Fax: +1-519-661-3613, E-mail: tschmitz@uwo.ca; Laszlo Zaborszky, Center for Molecular and Behavioral Neuroscience Rutgers University, 197 University Ave, Newark, NJ, United States. Tel: +1-973-353-3659, Fax: +1-973-353-1760, E-mail: laszloz@newark.rutgers.edu

Zaborszky et al., 2018; Sarter and Lustig, 2020). Paralleling the recent advances in basic research, there is renewed clinical research interest in the BF system as both a preclinical biomarker of neurodegenerative disease and as a target of therapeutic intervention (Hampel et al., 2018). Building on an extensive history of postmortem histology work dating from the 1980s, recent in vivo clinical neuroscience research on Alzheimer's and Parkinson's disease (AD and PD), has demonstrated that degeneration of the BF system is closely linked to cognitive impairments in both early AD (Grothe et al., 2010, 2012; Cantero et al., 2017; Scheef et al., 2019; Nemy et al., 2020) and PD (Ray et al., 2018; Schulz et al., 2018; Pereira et al., 2020). Emerging evidence suggests that structural degeneration of BF neurons occurs much earlier in these conditions than was previously thought, and may in fact precede, predict, and even potentiate cortical degeneration (Schmitz and Spreng, 2016; Schmitz et al., 2018; Fernandez-Cabello et al., 2020).

In the following, three sections of this chapter, we begin with a review of the first attempts to standardize the anatomy of the BF cholinergic system using nonhuman primate and rodent models. We then discuss more recent work in these nonhuman animal models, which has shed new light on the organizing principles of the cortical cholinergic projections, namely their cortical topography. In the second section of this chapter, we discuss recent in vivo neuroimaging work in humans, which has started to translate and extend the work from nonhuman animal models. This work shows that structural magnetic resonance imaging, functional MRI (fMRI), and vesicular acetylcholine transporter positron emission tomography (VAChT PET) are promising techniques for mapping the topography of the cholinergic projection system and deepening our understanding of its role in cognition. In the third and final section of this chapter, we discuss emerging evidence in human neuroimaging work indicating that the vulnerability of cholinergic BF neurons to aging and neurodegenerative disease also follows a subregional topography.

TOPOGRAPHIC PROJECTIONS OF THE BF IN RODENTS AND NONHUMAN PRIMATES

The nonhuman primate BF comprises a set of large hyperchromic neurons, also referred as magnocellular neurons, which provide the major cholinergic innervation to the cerebral cortex (Hedreen et al., 1984; Saper and Chelimsky, 1984; Mesulam and Geula, 1988). Early histology work showed that the majority of these magnocellular neurons project to large and discrete cortical regions, such as frontal, cingulate, and temporal cortices (Jones et al., 1976; Bigl et al., 1982; Pearson et al., 1983). More recent histology work has shown that this projection pattern reflects a topography of BF inputs and outputs (Zaborszky et al., 2015; Gielow and Zaborszky, 2017). The BF cholinergic neurons located more rostrally in the medial septum and the nucleus of the diagonal band of Broca project to the hippocampus, entorhinal cortex, olfactory bulb, and cingulate cortices (Mesulam and Van Hoesen, 1976; Pearson et al., 1983; Mesulam et al., 1983a; Zaborszky et al., 1986; Woolf, 1991; Kondo and Zaborszky, 2016). The BF cholinergic neurons located more caudally in the subcommissural and sublenticular substantia innominata, often referred to as the nucleus basalis of Meynert, project throughout the entire neocortex (Jones et al., 1976; Pearson et al., 1983; Mesulam et al., 1983a; Woolf, 1991) and to the amygdala (Carlsen et al., 1985).

In the early 1980s, Mesulam et al. introduced a "Ch" nomenclature that delineates *Ch*olinergic neurons based on their topography in the BF and their cortical targets in rodents (Mesulam et al., 1983b) and nonhuman primates (Mesulam et al., 1983a). Cholinergic cells in the medial septum and diagonal band of Broca that project to the hippocampus were designated as Ch1 and Ch2, respectively. The Ch3 group was used to refer a band of fusiform neurons that are close to the ventral surface of the brain in the subcommissural area and project to the olfactory bulb (Mesulam and Geula, 1988; Mufson et al., 1989). Those cholinergic cells projecting to the major part of the neocortex and amygdala were termed as Ch4.

Together, these early axonal tracing studies implied a rostro-caudal spatial topography of BF cholinergic innervation into the cortex and amygdala. More recent studies have shed further light on the anatomical significance of this topographic organization. Using retrograde tracers deposited into multiple frontal and posterior cortical areas of the rat brain, Zaborszky et al. (2015) demonstrated that labeled cells in the BF exhibit a complex topographic organization consisting of segregated and overlapping pools of projection neurons. The extent of this overlap seems to depend on the degree of connectivity between their cortical targets (Fig. 10.1). For example, BF cell populations projecting to cortical areas representing different body parts, such as S1 whisker and S1 hindlimb, have very low BF spatial overlap. In contrast, BF cell populations projecting to the primary somatosensory S1 and the corresponding primary motor M1 regions tend to have higher BF spatial overlap. This principle seems to extend to the level of individual BF neurons as well. Axonal branches from individual BF neurons innervate multiple cortical regions that are functionally related to one another, such as subregions of the prefrontal cortex (Chandler and Waterhouse, 2012; Chandler et al., 2013; Bloem et al., 2014; Chavez and Zaborszky, 2017). However, the branches of individual

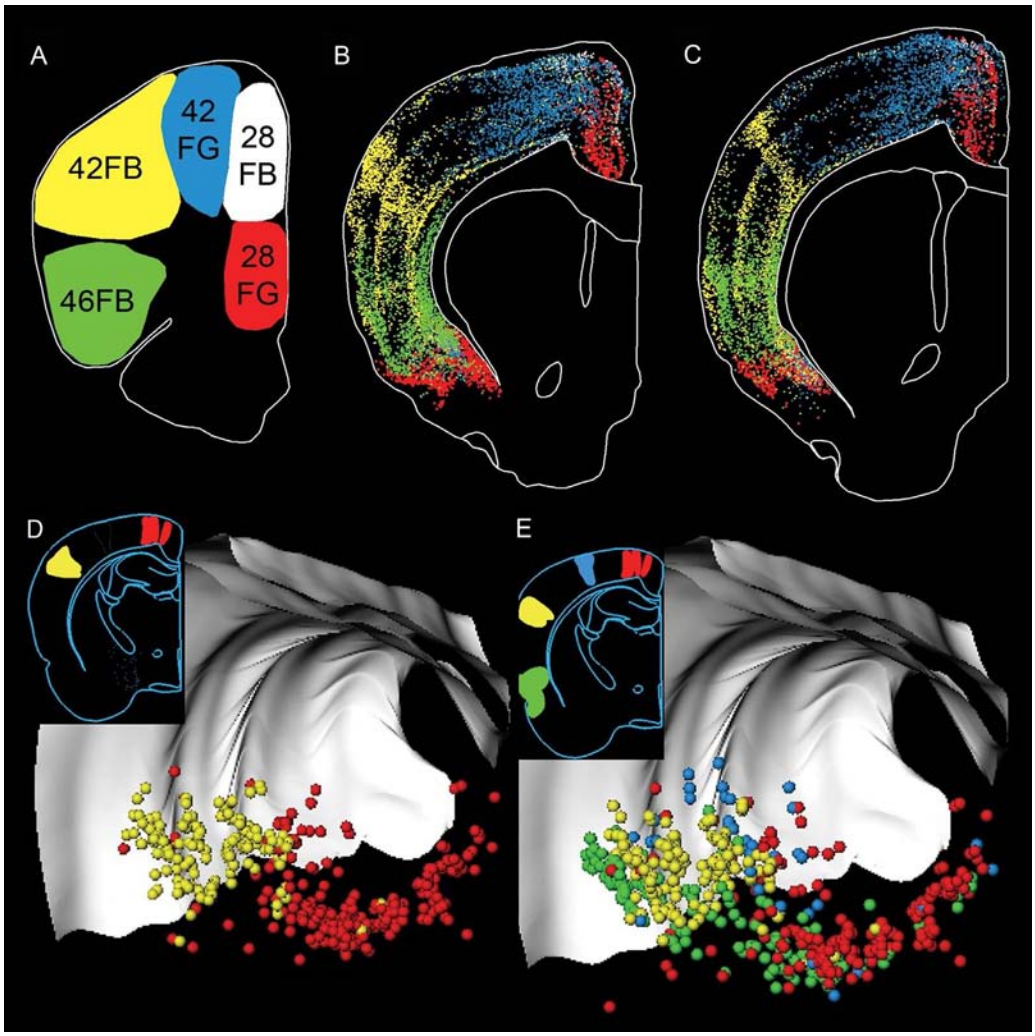

Fig. 10.1. A 3D rendering of the distribution of retrogradely labeled cells in the rat brain revealing the topographical organization of cortico-cortical (A–C) and basal forebrain (BF)-cortical (D, E) projections. When retrograde tracers are injected into different cortical locations (A), the organization of the cells in the posterior cortical areas that project to the frontal cortex becomes apparent (B and C: neurons are color coded according to their cortical injection site). The distribution of cortico-cortical projections has both rostro-caudal and medial-lateral organization. When retrograde tracers are injected into different cortical locations (D and E insets), the organization of the choline-o-acetyltransferase expressing (ChAT+) cholinergic cells in the BF that project to the frontal cortex becomes apparent (D, E: neurons are color coded according to their cortical injection site). The degree of overlap of BF neurons, as defined by their retrograde labeling from different locations in the frontal and posterior cortex (bottom row similarly colored clusters), is correlated with the amount of cortico-cortical connectivity of posterior cortical neurons, as defined by their retrograde labeling from different locations in frontal cortex (top row similarly colored clusters). Adapted from Zaborszky, L., Csordas, A., Mosca, K., et al., 2015a. Neurons in the basal forebrain project to the cortex in a complex topographic organization that reflects corticocortical connectivity patterns: an experimental study based on retrograde tracing and 3D reconstruction. Cereb Cortex 25, 118–137.

BF neurons do not appear to innervate functionally distinct regions of neocortex such as modality specific primary auditory A1 and primary visual V1 areas (Kim et al., 2016). Taken together, these results suggest a topographical organization of the BF projections at multiple spatial scales, from populations of BF neurons down to the axon branches of individual cells. This architecture appears well suited for coordinating information across the cortical hierarchy.

Despite these advances, the organizing principles of the mammalian BF cholinergic system and the functional properties embedded within its architecture are not fully worked out. There are three anatomical properties of the BF system that pose major challenges to its detailed experimental study: (1) the enormous and complex morphology of BF cholinergic neurons, (2) the multiplicity of postsynaptic cholinergic signaling pathways, and (3) the heterogeneity of noncholinergic neurons

codistributed within the BF. Nevertheless, genetically controlled techniques for cell-type specific labeling, stimulation, and receptor modeling are becoming available for studying the BF projection system at ever-increasing levels of precision (Letzkus et al., 2011; Arroyo et al., 2012; Pinto et al., 2013; Wu et al., 2014; Anaclet et al., 2015; Saunders et al., 2015; Unal et al., 2015; Xu et al., 2015; Do et al., 2016; Verhoog et al., 2016; Kuchibhotla et al., 2017; López-Hernández et al., 2017; Jing et al., 2018; Li et al., 2018; Laszlovszky et al., 2020). Although beyond the scope of this chapter, this work has demonstrated that the topography of the BF cholinergic system is expressed not only in terms of the input–output relationships of its cortical projections but also in the neurophysiological properties of cholinergic neurons across the rostral-caudal BF axis (Gielow and Zaborszky, 2017; Laszlovszky et al., 2020), the distributions of postsynaptic nicotinic and muscarinic cholinergic receptors in specific layers of the cortex (Verhoog et al., 2016), and the spatiotemporal dynamics of cortical state transitions (Pinto et al., 2013; Anaclet et al., 2015; Xu et al., 2015).

TOPOGRAPHIC PROJECTIONS OF THE BASAL FOREBRAIN IN HUMANS

Ex vivo localization of the human basal forebrain nuclei

Much less is understood about the organization of the human BF system compared to rodents and nonhuman primates. In human postmortem tissue samples, cholinergic BF neurons are often aggregated in clusters and constitute most of the large, or magnocellular, neurons (>20-μm-long axis) in this brain area. The delineation of these clusters on standard structural MRI is difficult to reproduce due to lack of specific landmarks, creating a major obstacle for in vivo neuroimaging of this structure.

However, the BF areas containing such magnocellular cell groups can be easily delineated in postmortem histological sections stained with a modified Gallyas's silver method for cell bodies (Merker, 1983). Using this approach, Zaborszky et al. (2008) identified clusters of hyperchromic magnocellular cell groups located close to the medial and ventral surfaces of the cerebral hemispheres (Fig. 10.2, left panels), including the septum,

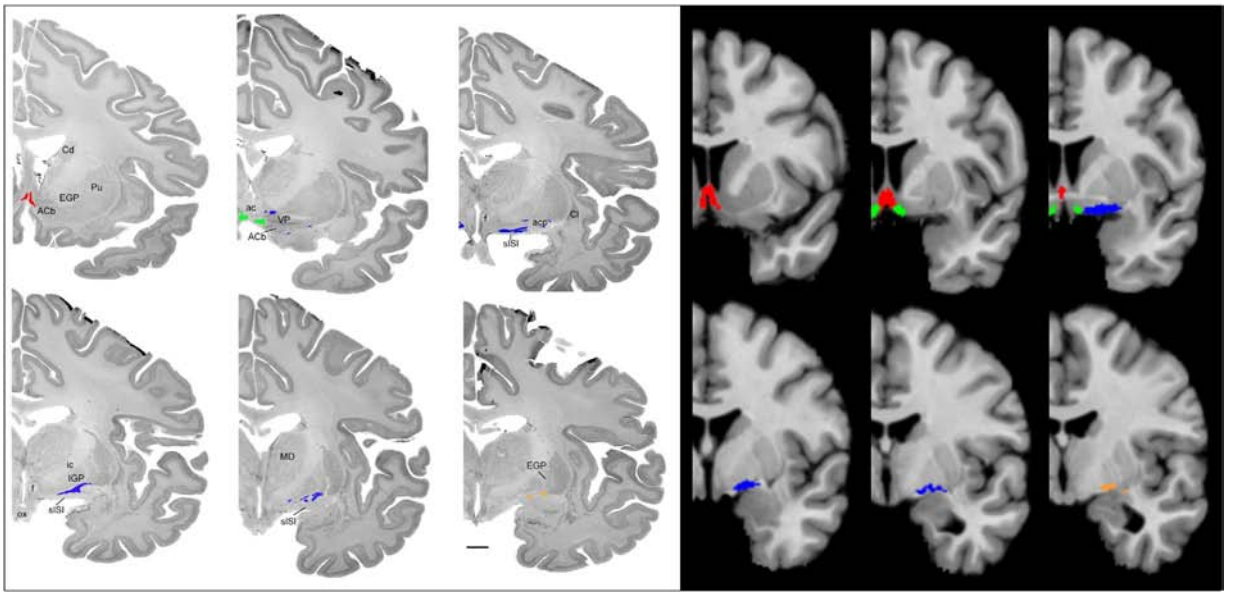

Fig. 10.2. Stereotaxic probabilistic maps of the human magnocellular basal forebrain (BF) space from Zaborszky et al. (2008) and Záborszky et al. (2015). *Left panels*: The BF space delineated on 2D images of silver-stained histological sections of a representative brain specimen. *Right panels*: The BF space after postmortem T1-weighted MRI scanning of 10 specimens, and coregistration into a common atlas space. The *colored areas* delineate the maximum probability maps of the various cholinergic (Ch) compartments: Ch12 (*red*, medial septal area, and vertical band of Broca), Ch3 (*green*, horizontal band of Broca), Ch4 (*blue*, nucleus basalis of Meynert), and Chp (*orange*, nucleus of Ayala). A voxel was assigned to a BF area that showed the greatest overlap (winner take all) among the 10 examined postmortem brains or that exceeded a threshold of 40% probability (4/10 brain overlapped). As a result, maximum probability maps show a nonoverlapping representation of the Ch compartments in the Montreal Neurological Institute anatomical template space. *ACb*, nucleus accumbens; *ac*, anterior commissure; *Cd*, caudate nucleus; *Cl*, claustrum; *EGP*, external globus pallidus; *IGP*, internal globus pallidus; *ic*, internal capsule; *ox*, optic chiasm; *Pu*, putamen.

the horizontal and vertical limbs of the diagonal band, the basal nucleus of Meynert, and cell groups interspersed in the so-called "extended amygdala" (the area underneath the globus pallidus bridging the centromedial amygdala to the bed nucleus of the stria terminalis). Following from Mesulam's "Ch" nomenclature for cholinergic compartments (Mesulam et al., 1983a, b), Zaborszky et al. (2008) separated these groups into medial septal and vertical band of Broca (Ch1 and Ch2, Red), the horizontal band of Broca (Ch3, Green), the nucleus basalis of Meynert (Ch4, Blue), and a posterior group behind the supraoptic nucleus, where the optic tract attaches to the internal capsule/cerebral peduncle, including the nucleus of Ayala (Ch4p, Orange).

Other atlases of the human BF Ch space have also been produced in single brain specimens using similar procedures to Zaborszky and colleagues (Teipel et al., 2005; Kilimann et al., 2014). Unlike these atlases, however, Zaborszky et al. (2008) delineated BF Ch groups in a total of 10 postmortem brains that were then digitized and coregistered into the MNI single-subject reference brain (Colin27) as a common brain atlas space, allowing the creation of a probabilistic anatomical map of the human BF compartments (Fig. 10.2, right panels). Since postmortem probabilistic maps were constructed primarily based on the presence of large neurons that are mostly cholinergic, the BF space is referred to as the BF cholinergic space. The probabilistic human BF atlas can be thresholded to infer the location of the Ch compartments at varying levels of certainty, e.g., a 50% probability threshold isolates voxels that converge on a given BF Ch compartment in 5/10 brains. However, unlike studies in nonhuman animal models (Fig. 10.1), it should be noted that the human subdivisions are defined without reference to projection targets or cell-type specific labeling.

Similar postmortem histology approaches have been taken to map the projections of the human cholinergic BF. Selden et al. (1998) used acetylcholinesterase (AChE) histochemistry to trace AChE-rich white matter fibers originating from the nucleus basalis of Meynert or Ch4 (Fig. 10.3). Consistent with a topographical organization of BF projections, they identified two primary pathways originating from Ch4 (blue). A medial pathway (green) traveled within the cingulum to supply the orbitofrontal, subcallosal, cingulate, pericingulate, and retrosplenial cortices. A lateral pathway subdivided into a capsular (red) and perisylvian (orange) component. The capsular pathway traveled within the external capsule and uncinate fasciculus to supply the putamen, amygdala, middle, and inferior temporal gyri, parahippocampal gyri, and dorsal frontoparietal neocortex. The perisylvian component traveled within the claustrum to supply the insula, superior temporal gyri, and ventral (opercular) frontoparietal neocortex. The more rostral BF Ch compartments, including Ch1–3, were not assessed in this study. To date, the immunohistochemical mapping of the human BF cholinergic projection system remains incomplete.

In vivo MRI of the human basal forebrain nuclei and topographic projections

Taken together, the atlases of the BF Ch compartments and their projections serve a common purpose, which is to provide anatomically defined landmarks for structural and functional neuroimaging experiments. We review some of these applications in this section and in section "Spatial Topography of Basal Forebrain Vulnerability to Neurodegeneration."

Several different research groups have used resting-state functional MRI data to validate the anatomical parcellation of the BF Ch compartments and evaluate the topographical organization of their projections (Figs. 10.2 and 10.3). These studies capitalize on spontaneous fluctuations in hemodynamic responses measured from individual voxels, the smallest unit of measurement in MRI brain volumes. By measuring these fluctuations at each voxel in the brain over a sequence of several hundred timepoints acquired every ~2 s, one can determine whether fluctuations in different voxels correlate with one another over time (Li et al., 2014; Kline et al., 2016; Teipel et al., 2017; Zhang et al., 2017; Markello et al., 2018; Fritz et al., 2019; Yuan et al., 2019). These voxel-wise correlations can be used to determine whether brain regions exhibit spatial clustering of correlated spontaneous fluctuations, i.e., different groups or parcels of neighboring voxels with shared connectivity profiles.

Yuan et al. (2019) used high-resolution 7 T functional MRI to parcel the entire Ch1–Ch4 BF volume based on clusters of voxels exhibiting correlated spontaneous fluctuations in resting-state hemodynamic responses. Consistent with a topographic organization, voxels within the BF masking area grouped into three distinct clusters based on the strength of their correlated hemodynamic fluctuations (Fig. 10.4A). These data-driven functional parcels combined areas Ch1, Ch2, and Ch3 mask all together into Cluster 1, the anterior part of the Ch4 masks into Cluster 2, and the posterior Ch4p into Cluster 3. These three clusters exhibited both overlapping and distinct functional connectivity profiles with different resting-state networks (Fig. 10.4B). For instance, all clusters showed connectivity with salience networks. Cluster 1 was significantly associated with the default mode network, posterior default mode, salience network, auditory and language networks, as well as premotor (precentral) network. Cluster 2 was significantly connected with the salience, attention, language, and

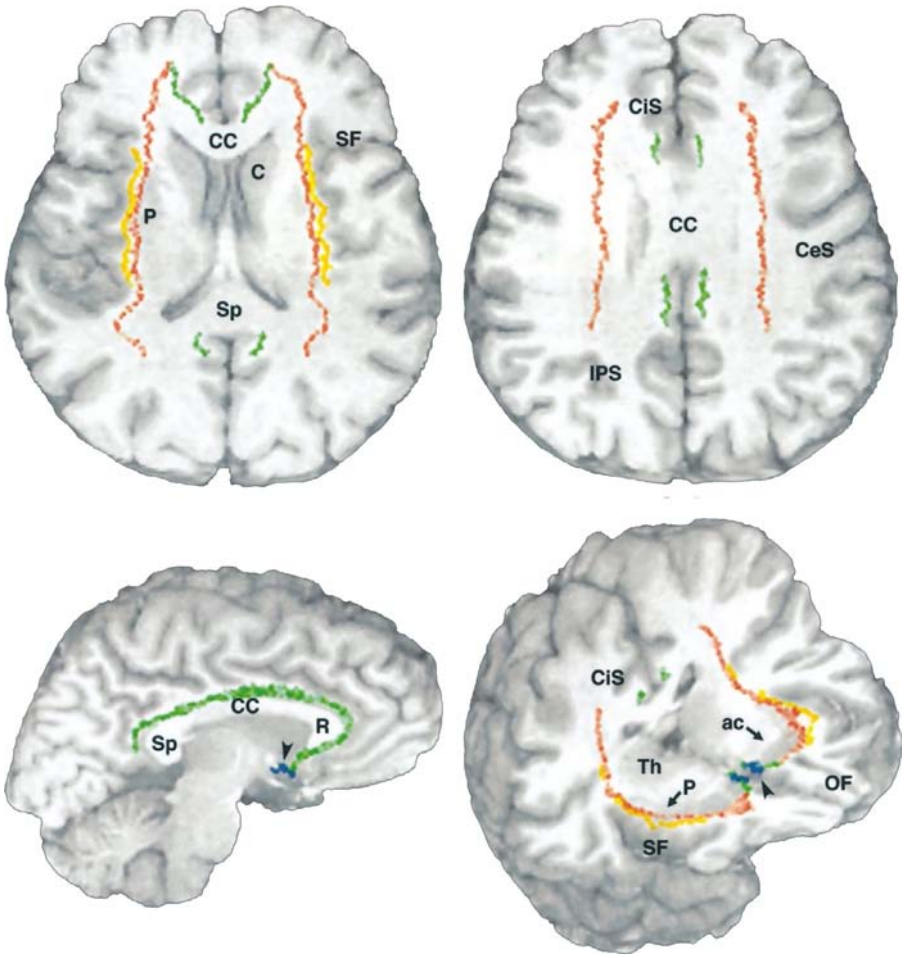

Fig. 10.3. Acetylcholinesterase (AChE) histochemistry was used to identify AChE-rich white matter fibers originating from the nucleus basalis of Meynert (equivalent to area Ch4 in Fig. 10.2) in five postmortem human brains. The locations of these projections in anatomical sections were traced onto a single-subject T1-weighted MRI volume. Cholinergic fiber bundles originating from the Ch4 region (*blue*) formed a medial pathway traveling within the cingulum (*green*) and a lateral pathway which further subdivided into a capsular component traveling within the external capsule and uncinate fasciculus (*red*), and a perisylvian component traveling within the claustrum (*orange*). The arrowhead points to the Ch4 neurons which give rise to the corticopetal cholinergic pathways. *ac*, anterior commissure; *C*, caudate; *CC*, corpus callosum; *CeS*, central sulcus; *CiS*, cingulate sulcus; *IPS*, intraparietal sulcus; *OF*, orbitofrontal cortex; *P*, putamen; *R*, rostrum of corpus callosum; *SF*, Sylvian fissure; *Sp*, splenium of corpus callosum; *Th*, thalamus. Adapted from Selden, N.R., Gitelman, D.R., Mesulam, M.-M., 1998. Trajectories of corticopetal cholinergic pathways within the cerebral hemispheres of the human brain NeuroImage, 7, S26.

premotor networks. Cluster 3 was preferentially correlated with the sensory-motor, premotor, attention, salience, and auditory networks.

Using independent resting-state fMRI datasets, Fritz et al. (2019) recovered highly similar three-cluster parcellations and connectivity maps for the BF. Taken together, the resting-state parcellations of the BF indicate that correlated fluctuations in hemodynamic response can provide reliable estimates of subregional BF connectivity.

In vivo structural MRI can also be used to measure the brain's white matter microstructure. In particular, diffusion tensor imaging measures the rate of water diffusion along axon bundles in the white matter. Diffusion tensor tractography can then be used to infer the principal direction of this water diffusion and thus the white matter connectivity of "streamlines" between distal regions of the brain. Tractography has been used to evaluate the topography of white matter projections in the BF nucleus basalis of Meynert (Ch4) in living humans (Liu et al., 2017; Nemy et al., 2020), guided by the postmortem work of Selden et al. (1998). These two in vivo imaging studies recovered medial and lateral white matter Ch4 pathways that largely resemble those identified postmortem by Selden et al. (1998), indicating that diffusion tractography is a promising tool for further evaluating the BF projectome. A complete mapping of the human

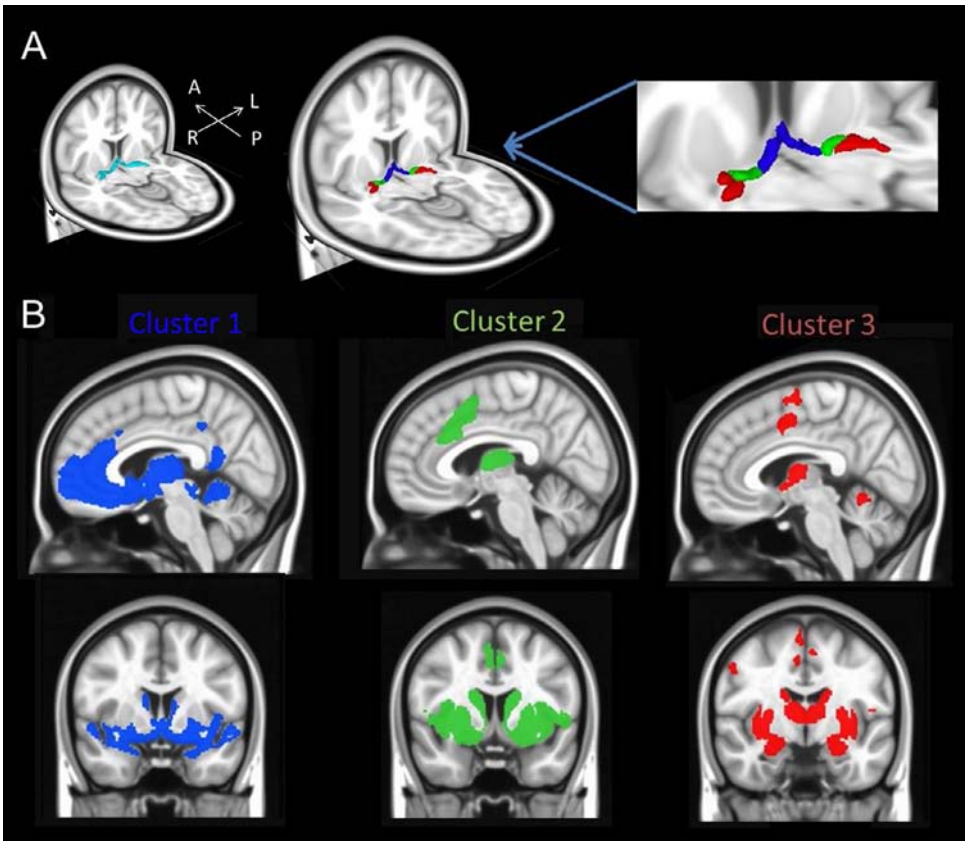

Fig. 10.4. Parcellation of the human cholinergic BF and its projections from 7 T resting-state fMRI. (A) *Left*: The light blue region of interest corresponds to the anatomical BF atlas (Fig. 10.2). *Right*: Voxels colocalized with the basal forebrain (BF) cholinergic (Ch) compartments grouped into three distinct clusters based on the strength of their correlated hemodynamic fluctuations. These data-driven functional parcels combined areas Ch1, Ch2, and Ch3 masks all together into Cluster 1, the anterior part of the Ch4 mask into Cluster 2, and the posterior Ch4p into Cluster 3. (B) These three clusters exhibited both overlapping and distinct functional connectivity profiles with other brain areas. Adapted from Yuan, R., Biswal, B.B., Zaborszky, L., 2019. Functional subdivisions of magnocellular cell groups in human basal forebrain: test–retest resting-state study at ultra-high field, and meta-analysis. Cerebral Cortex Oxford Academic, 29, 2844–2858.

BF projectome, integrating ex vivo and in vivo datasets with coverage of the entire set of Ch compartments (Ch1-4p) is lacking.

Because in vivo MRI techniques such as resting-state functional MRI and diffusion tensor imaging lack cell-type specificity, the ability to differentiate BF cholinergic compartments and their projections from other intermingled neurons represents a major methodological challenge. For example, we cannot infer from standard T1-weighted MRI assays of bulk gray and white matter tissue whether the tissue localized by the BF Ch compartments are specific to cholinergic cells or some combination of other cell types known to copopulate this region (Brashear et al., 1986; Freund and Gulyás, 1991; Freund and Meskenaite, 1992; Gritti et al., 1993, 2003, 2006; Hur and Zaborszky, 2005; Henny and Jones, 2008; Lin et al., 2015). Moreover, the interpretation of BF functional and structural connectivity patterns is complicated by the fact that these indices likely reflect both monosynaptic and polysynaptic anterograde and retrograde connections (Skudlarski et al., 2008; Honey et al., 2009).

In vivo PET of the human basal forebrain compartments and projections

Positron emission tomography (PET) is emerging as a promising tool for cell-type specific imaging of cholinergic projections in the living human brain. There are multiple PET radiotracers for imaging the cholinergic system, including radiotracers which bind to nicotinic (Horti et al., 2010) and muscarinic receptors (Malmquist et al., 2018), as well as the enzyme acetylcholinesterase (Kikuchi et al., 2013; Richter et al., 2018, 2019). A full review of these postsynaptic radiotracers and their ongoing development for clinical use is beyond the scope of this chapter. Here, we focus on a well-established PET radiotracer for imaging the presynaptic cholinergic system: ^{18}F-fluoroethoxybenzovesamicol

([^{18}F] FEOBV) (Mulholland et al., 1998); see also Tu et al. (2015) for a chemically similar radiotracer ([^{18}F] VAT).

The [^{18}F] FEOBV radiotracer binds with high sensitivity and specificity to the vesicular acetylcholine transporter (VAChT), a glycoprotein which is expressed in all presynaptic cholinergic nerve terminals of the mammalian central nervous system. Consistent with a topographic organization of cholinergic projections, experimentally induced lesions of cholinergic neurons in rats selectively reduces [^{18}F] FEOBV binding in the subcortical and cortical areas receiving their projections (Parent et al., 2012; Cyr et al., 2014). More recently, a first-in-human in vivo [^{18}F] FEOBV PET study (Aghourian et al., 2017) provided a whole brain cell-type specific map of brain areas that receive cholinergic input. This study also demonstrated that [^{18}F] FEOBV was decreased in the brains of cognitively impaired patients with probable AD (confirmed by a separate PET scan of amyloid binding). Further work in cognitively normal young and older adult humans has shown that [^{18}F] FEOBV PET is sensitive to age-related changes in central cholinergic integrity (Albin et al., 2018). In these studies, the observed spatial distribution of [^{18}F] FEOBV binding throughout the brain closely mirrors the expected spatial distribution of the cholinergic projection zones based on prior anatomical studies (Fig. 10.5). Collectively, these findings suggest that PET imaging of presynaptic VAChT expression might serve as a powerful complementary approach to MRI methods for basic neuroscience research examining the topographical organization of the BF cholinergic system.

SPATIAL TOPOGRAPHY OF BASAL FOREBRAIN VULNERABILITY TO NEURODEGENERATION

The development of digital atlases for the BF cholinergic space (Teipel et al., 2005; Zaborszky et al., 2008; Kilimann et al., 2014) opened the way to investigate how in vivo structural changes in BF compartments correlate with topography of cortical pathology and progression of cognitive symptoms in neurodegenerative diseases of aging. In combination with the availability of large multimodal longitudinal neuroimaging datasets, such as the Alzheimer's Disease Neuroimaging Initiative (Mueller et al., 2005) and Parkinson's progressive markers initiative (Schrag et al., 2017), there has been a resurgence of interest in and evidence for the primacy of the cholinergic lesion in age-related neurodegenerative disease such as AD, and more recently, in PD. Later we review some of the work over the past 10 years which has combined probabilistic mapping of the human BF with in vivo neuroimaging, neuropsychological, and biospecimen data to examine subregional neurodegeneration of this structure in AD and PD.

Topography of basal forebrain vulnerability in Alzheimer's disease

Several cross-sectional structural MRI studies evaluating gray matter volume within the predefined BF atlas (e.g., Fig. 10.6) have consistently found evidence that subregional degeneration is not uniformly distributed across the Ch compartments in clinically diagnosed MCI and AD patients compared to age-matched controls (Teipel et al., 2005, 2011; Grothe et al., 2010, 2012; Kilimann et al., 2014; Cantero et al., 2017, 2020). These studies show that the posterolateral Ch4 and especially Ch4p BF compartments exhibit larger magnitudes of gray matter loss in MCI-AD compared to the more anteromedial Ch1–3 compartments (Fig. 10.6). By incorporating cerebrospinal fluid biomarkers of amyloid and tau as staging criteria, more recent cross-sectional studies have demonstrated the caudo-rostral axis of BF vulnerability at even earlier "preclinical" stages of AD, e.g., in cognitively normal adults with abnormal cerebrospinal fluid biomarkers of tau pathology (Cantero et al., 2020).

Studies which leverage both longitudinal structural MRI and cerebrospinal fluid biomarkers of amyloid-beta and tau neuropathology as staging criteria have enabled still further sensitivity to the cholinergic BF lesion in AD (Schmitz and Spreng, 2016; Schmitz et al., 2018, 2020; Fernandez-Cabello et al., 2020). These studies showed that annual rates of gray matter loss in the Ch4 and Chp BF subregion are detectable in cognitively normal older adults with abnormal cerebrospinal fluid biomarkers of amyloid and tau pathology. Moreover, degeneration of Ch4/Ch4p was consistently found to both precede and predict longitudinal degeneration in other vulnerable brain areas associated with the earliest phases of AD, such as the entorhinal, transentorhinal and perirhinal cortices. For instance, Fernandez-Cabello et al., 2020 showed that the Ch4/Ch4p→entorhinal predictive staging pattern of neurodegenerative spread is replicable between two large independent samples of older adults tracked over 2 years with longitudinal MRI. The strength of this pattern was significantly increased among older adults with abnormal CSF amyloid-beta and tau markers of neuropathology (Fig. 10.7A).

Follow-up exploratory whole brain staging models (not restricted to the entorhinal cortical region of interest) revealed that the medial temporal lobe structure most strongly expressing the predictive relationship from BF Ch4/Ch4p was in the adjacent transentorhinal region (Fig. 10.7B). These findings map well with known routes of BF cholinergic projections in rodent models, which show that the entorhinal cortex receives projections from the rostral Ch compartment, and the perirhinal cortex (Brodmann area 35) receives cholinergic projections from the caudal Ch compartment (Kondo and Zaborszky,

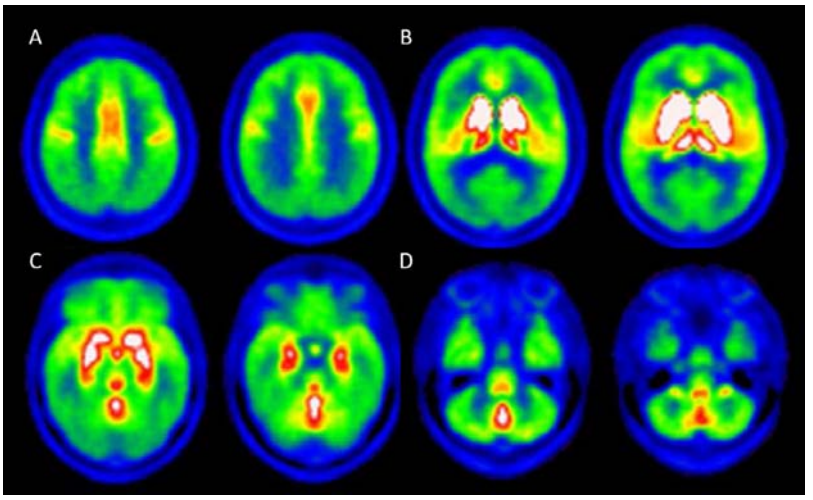

Fig. 10.5. PET imaging of the cholinergic projection system with [^{18}F] FEOBV (average of 13 young adults, mean age: 25 years, range: 20–38 years). The radiotracer binds to the vesicular acetylcholine transporter (VAChT) glycoprotein, which is expressed selectively on the presynaptic nerve terminals of intrinsic cholinergic neurons. (A and B) Axial slices showing higher [^{18}F] FEOBV PET binding (*warmer colors*; *white maximum*) in units of standard uptake value ratio (SUVR) relative to the white matter. Each panel shows two closely situated slices in descending order (superior to inferior). (A) Neocortical binding sites in anterior cingulate and supplementary motor areas. (B) Dorsal striatal binding sites in the caudate nucleus and putamen, extending to the globus pallidus and thalamus. (C) Ventral striatal and pallidal binding sites (nucleus accumbens and basal forebrain), amygdala, hippocampus, and entorhinal cortex. (D) Mesopontine and cerebellar binding sites in tegmental nuclei, vermis, and flocculus. Figure adapted from Albin, R.L., Bohnen, N.I., Muller, M.L., et al., 2018. Regional vesicular acetylcholine transporter distribution in human brain: a [18F] fluoroethoxybenzovesamicol positron emission tomography study. J Comp Neurol Wiley Online Library, 526, 2884–2897.

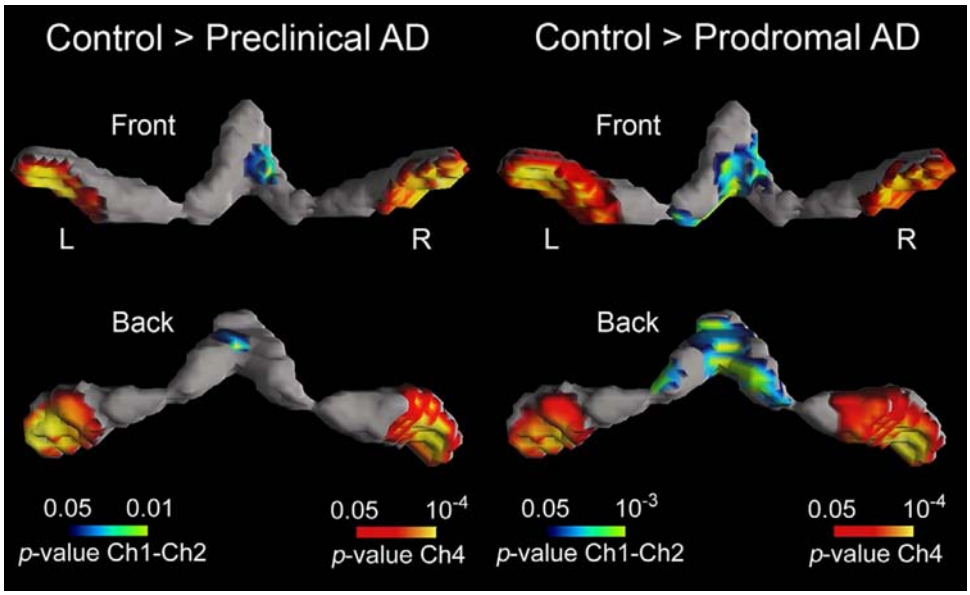

Fig. 10.6. Subregional degeneration of the BF in cognitively normal neurotypical older adults compared to preclinical adults (*left side*) and prodromal adults (*right side*). Preclinical status was defined as cognitively normal with abnormal cerebrospinal fluid biomarkers of amyloid and tau. Prodromal status was defined as mild cognitive impairment with abnormal cerebrospinal fluid biomarkers of amyloid and tau. In earlier (preclinical) stages of AD, subregional BF degeneration is stronger in posterolateral Ch4/Ch4p compartments (*warm clusters*) compared to anteromedial Ch1–3 compartments (*cool clusters*). *AD*, Alzheimer's disease; *Ch*, cholinergic cells. Adapted from Cantero, J.L., Atienza, M., Lage, C., et al., 2020. Atrophy of basal forebrain initiates with tau pathology in individuals at risk for Alzheimer's disease. Cereb Cortex 30, 2083–2098.

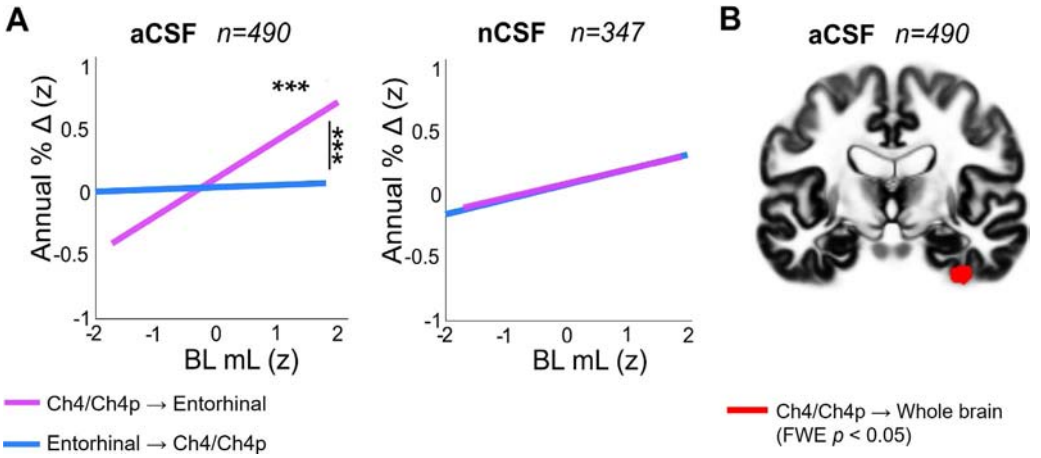

Fig. 10.7. Baseline gray matter volume (*x*-axes: BL mL = baseline milliliters) predicting subsequent longitudinal change in gray matter volume (*y*-axes: annual percent change in gray matter volume over 2 years, follow-up—baseline). (A) A priori region of interest analyses in BF Ch4/4p and entorhinal cortex. (*Left plot*) Baseline BF Ch4/4p gray matter volume predicts longitudinal change in entorhinal gray matter volume (*magenta*) more strongly compared to the reverse model (*blue*). The Ch4/4p → Entorhinal relationship was stronger among older adults with abnormal cerebrospinal fluid biomarkers of amyloid and phosphorylated tau pathology (aCSF, $n = 490$ adults). (*Right plot*) No difference between models was detected in older adults with normal CSF levels of amyloid and phosphorylated tau pathology (nCSF, $n = 347$ adults). (B) Exploratory whole brain analysis. When examining where baseline BF Ch4/4p gray matter volume predicts longitudinal changes in whole brain gray matter volume, suprathreshold voxels are restricted to the transentorhinal cortex (family-wise error corrected $P < 0.05$). *Annual % Δ*, annualized percent change in gray matter volume; *aCSF*, abnormal cerebrospinal fluid ratio of amyloid-beta concentration over phosphorylated tau concentration; *BL mL*, baseline gray matter volume in milliliters; *FWE*, family-wise error corrected *P*-value; *nCSF*, normal cerebrospinal fluid ratio of amyloid-beta concentration over phosphorylated tau concentration. Adapted from Fernandez-Cabello, S., Kronbichler, M., Van Dijk, K.R.A., et al., 2020. Basal forebrain volume reliably predicts the cortical spread of Alzheimer's degeneration. Brain 143, 993–1009.

2016). In humans, this corresponds to the transentorhinal area, through which, like a funnel, the various neocortical areas project to the hippocampus. Disruption of cholinergic transmission in the transentorhinal/perirhinal cortices impairs object recognition (Tang et al., 1997; Winters et al., 2004). The emergence of localized tau pathology in human postmortem histological samples isolates cortical Stage 1 in the Braak predictive pathological staging model of AD (Braak and Del Tredici, 2015). The findings of Fernandez-Cabello et al. (2020) indicate that loss of Ch4/4p structural integrity precedes and predicts transentorhinal/entorhinal cortical degeneration, though higher resolution structural MRI data will be necessary to more conclusively disambiguate patterns of gray matter loss in these closely situated areas.

As mentioned in section "Topographic Projections of the Basal Forebrain in Humans," the use of MRI data to delineate neurobiologically grounded topographic relationships between the BF and cortex requires multiple assumptions. One major assumption is that the interregional relationships in bulk gray and white matter structure observed between BF compartments and other brain areas reflect cholinergic projections. Multimodal imaging, integrating structural MRI, and [^{18}F] FEOBV provides initial clues in support of this assumption (Schmitz et al., 2018). Patterns of longitudinal gray matter loss in the brain, assessed from structural MRI, tend to overlap patterns of cholinergic denervation assessed from [^{18}F] FEOBV PET (Fig. 10.8), implying that some proportion of cortical degeneration might reflect spatial topographies of cholinergic denervation. More work is needed to examine the interplay and timing of cholinergic denervation with the molecular and structural neuroimaging markers of AD pathology.

Topography of basal forebrain vulnerability in Parkinson's and dementia with Lewy bodies

Pronounced BF cholinergic degeneration is observed in PD patients with dementia (PDD) and in patients with Lewy body dementia (LBD). Alpha-synuclein proteinopathy, which is common to PD, PDD, and LBD (Spillantini et al., 1997), may therefore also contribute to BF cholinergic degeneration. However, like amyloid and tau proteinopathies in AD, the causal mechanisms of BF cholinergic degeneration remain to be determined. Later we review some of the emerging evidence of an early BF cholinergic lesion in PDD and LBD.

The "dual-syndrome" hypothesis of PD (Williams-Gray et al., 2009, 2013; Kehagia et al., 2013) proposes

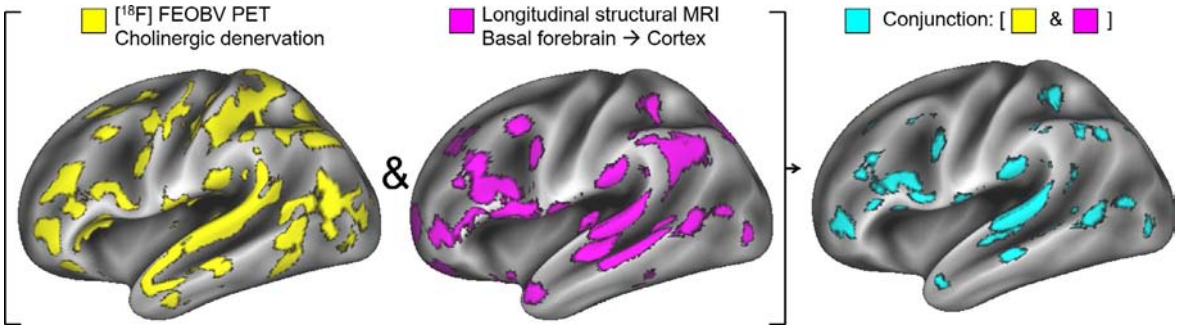

Fig. 10.8. From left to right, each cortical surface depicts a different measure of degeneration in the cholinergic systems of living older adult humans. (*Left*) Positron emission tomography (PET) was used in combination with the radiotracer [^{18}F] FEOBV, which binds to the cortical terminals of cholinergic neurons in the brain. Radiotracer binding intensity was reduced in older adults with early Alzheimer's disease (AD) compared to cognitively normal controls, indicating substantial loss of cholinergic terminals in the cortex (*yellow clusters*). (*Middle*) Magnetic resonance imaging (MRI) was used to measure changes in gray matter volume in the brain over a period of 2 years. Across individuals with early AD, loss of gray matter volume in the basal forebrain tracked with loss of gray matter volume in certain areas of the cortex (*purple clusters*). (*Right*) A "conjunction" map of the PET and MRI indices of cholinergic degeneration (left and middle panels, respectively) detected substantial overlap between these two distinct measures. Adapted from Schmitz, T.W., Mur, M., Aghourian, M., et al., 2018. Longitudinal Alzheimer's degeneration reflects the spatial topography of cholinergic basal forebrain projections. Cell Rep 24, 38–46.

that there are two phenotypes of PD with potentially distinct genetic contributions. The first PD phenotype is characterized by degeneration of dopaminergic neurons located in the substantia nigra pars compacta, the consequent loss of dopaminergic innervation in fronto-striatal circuits, and executive impairments. Patients exhibiting the dopaminergic PD phenotype respond well to dopaminergic agonists and typically do not progress to dementia. The second PD phenotype is characterized by memory and visuospatial impairments that rapidly progress to dementia, i.e., PDD. Patients with this neuropsychological profile respond well to the same classes of drugs used to treat AD, namely the acetylcholinesterase inhibitors, implying that PDD may represent a distinct cholinergic PD phenotype.

Following from the prediction that PDD should more strongly predict BF cholinergic degeneration than PD without dementia, Ray et al. (2018) used structural MRI to classify newly diagnosed cognitively normal PD patients into two groups based on MRI measures of their BF volume. This strategy produced two subgroups of PD patients, a control group and a group with abnormally small BF volume (one standard deviation below controls). They then tracked cognitive changes in these individuals over 5 years. Consistent with the dual-syndrome hypothesis, PD patients with smaller BF volumes on their baseline MRI scan showed greater decline on measures of recall memory and semantic fluency compared to control PD patients, implying greater temporoparietal degeneration. The groups declined at similar rates on measures of executive function. Other structural MRI studies have since shown that the cholinergic PDD phenotype, like AD, preferentially impacts gray matter loss in the posterolateral Ch4/Ch4p BF compartments over the anteromedial C1/Ch2 compartments (Schulz et al., 2018; Pereira et al., 2020).

LBD is distinguished from PDD based on the clinical onset of cognitive symptoms relative to motor symptoms (cognitive precede motor deficits in LBD and vice versa in PDD). Nejad-Davarani et al. (2019) examined LBD patients with [^{18}F] FEOBV PET and observed evidence of a pronounced loss in cholinergic innervation throughout the brain. Due to the limited spatial resolution of PET, subregional BF analyses were not performed in that study. Nevertheless, these collective findings imply that AD, PDD, and LBD may share a common pathophysiological basis linked to early degeneration of the posterolateral BF cholinergic system.

Selective neuronal vulnerability to neurodegeneration: Factors and future directions

If the posterolateral BF cholinergic cell, populations degenerate earlier than anteromedial populations in certain neurodegenerative diseases; we need to understand why this is so. The factors contributing to a local topography of degeneration in the BF may reveal important insights into cellular organization and vulnerability. The posterolateral and anteromedial cholinergic cell groups are thought to arise from distinct progenitors (Semba and Fibiger, 1988; Koh and Loy, 1989; De Carlos et al., 1995). Neurogenesis of the posterolateral cell populations occurs earlier in the developing rodent brain compared to

the anteromedial cell populations (Semba and Fibiger, 1988). Projections from the posterolateral cell populations into lateral and medial cortices also arrive earlier than the anteromedial projections into the hippocampus (De Carlos et al., 1995). In line with the possibility of distinct germinal sources, transcriptional (Pombero et al., 2011) and electrophysiological (Laszlovszky et al., 2020) profiling of mouse BF cholinergic neurons indicates that the posterolateral and anteromedial populations have distinct molecular properties and functional roles. Clues to posterolateral cholinergic BF vulnerability might therefore be gleaned from a deeper understanding of their ontogeny.

Moving from basic to clinical neuroscience, abnormal posterolateral BF cholinergic degeneration appears to identify three populations of cognitively normal at-risk individuals: (1) those with amyloid and tau pathology who progress to Alzheimer's dementia, (2) those with alpha-synuclein pathology who progress to Parkinson's dementia, and (3) possibly those with alpha-synuclein pathology who progress to Lewy body dementia. For the neurologist, this presents both challenges and opportunities. Current diagnostic criteria are usually based on *whether* there are cognitive symptoms in addition to motor symptoms (this differentiates AD from LBD and PD) or *when* cognitive symptoms started relative to the onset of motor symptoms (this differentiates LBD from PD). However, in all three cases, there is a long preclinical window of posterolateral BF cholinergic degeneration, which precedes the emergence of early cognitive symptoms. After the emergence of early cognitive symptoms, continued degeneration of the posterolateral BF is closely related to the progression to dementia. Because clinical diagnoses are tethered to the onset of early to moderate cognitive symptoms in AD and LBD, preclinical stages of these two neurodegenerative diseases, possibly spanning up to a decade, are currently beyond the reach of clinical treatment.

With the continued development of biomarkers sensitive to BF cholinergic integrity, future translational research bridging basic and clinical neuroscience is poised to facilitate dramatic improvements in preclinical identification of at-risk AD and LBD patients, as well as identification of de novo PD patients at-risk for dementia. In turn, drugs aimed at protecting the vulnerabilities of posterolateral BF cholinergic neurons in the preclinical window represent a highly promising strategy for preventing dementia in at-risk older adults.

ACKNOWLEDGMENTS

This work was financially supported by a Natural Sciences and Engineering Research Council of Canada (NSERC) grant to T.W.S. and a National Institute of Health NIH/NINDS 2RF1NS023945-28 to L.Z.

References

Aghourian M, Legault-Denis C, Soucy JP et al. (2017). Quantification of brain cholinergic denervation in Alzheimer's disease using PET imaging with [18F]-FEOBV. Mol Psychiatry 11: 1531–1538.

Albin RL, Bohnen NI, Muller ML et al. (2018). Regional vesicular acetylcholine transporter distribution in human brain: A [18F] fluoroethoxybenzovesamicol positron emission tomography study. J Comp Neurol 526: 2884–2897.

Anaclet C, Pedersen NP, Ferrari LL et al. (2015). Basal forebrain control of wakefulness and cortical rhythms. Nat Commun 6: 8744.

Arroyo S, Bennett C, Aziz D et al. (2012). Prolonged disynaptic inhibition in the cortex mediated by slow, non-α7 nicotinic excitation of a specific subset of cortical interneurons. J Neurosci 32: 3859–3864.

Ballinger EC, Ananth M, Talmage DA et al. (2016). Basal forebrain cholinergic circuits and signaling in cognition and cognitive decline. Neuron 91: 1199–1218.

Bigl V, Woolf NJ, Butcher LL (1982). Cholinergic projections from the basal forebrain to frontal, parietal, temporal, occipital, and cingulate cortices: a combined fluorescent tracer and acetylcholinesterase analysis. Brain Res Bull 8: 727–749.

Bloem B, Schoppink L, Rotaru DC et al. (2014). Topographic mapping between basal forebrain cholinergic neurons and the medial prefrontal cortex in mice. J Neurosci 34: 16234–16246.

Braak H, Del Tredici K (2015). The preclinical phase of the pathological process underlying sporadic Alzheimer's disease. Brain 138: 2814–2833.

Brashear HR, Zaborszky L, Heimer L (1986). Distribution of GABAergic and cholinergic neurons in the rat diagonal band. Neuroscience 17: 439–451.

Cantero JL, Zaborszky L, Atienza M (2017). Volume loss of the nucleus basalis of Meynert is associated with atrophy of innervated regions in mild cognitive impairment. Cereb Cortex 27: 3881–3889.

Cantero JL, Atienza M, Lage C et al. (2020). Atrophy of basal forebrain initiates with tau pathology in individuals at risk for Alzheimer's disease. Cereb Cortex 30: 2083–2098.

Carlsen J, Záborszky L, Heimer L (1985). Cholinergic projections from the basal forebrain to the basolateral amygdaloid complex: a combined retrograde fluorescent and immunohistochemical study. J Comp Neurol 234: 155–167.

Chandler D, Waterhouse BD (2012). Evidence for broad versus segregated projections from cholinergic and noradrenergic nuclei to functionally and anatomically discrete subregions of prefrontal cortex. Front Behav Neurosci 6: 20.

Chandler DJ, Lamperski CS, Waterhouse BD (2013). Identification and distribution of projections from monoaminergic and cholinergic nuclei to functionally differentiated subregions of prefrontal cortex. Brain Res 1522: 38–58.

Chavez C, Zaborszky L (2017). Basal forebrain cholinergic-auditory cortical network: primary versus nonprimary auditory cortical areas. Cereb Cortex 27: 2335–2347.

Cyr M, Parent MJ, Mechawar N et al. (2014). PET imaging with [^{18}F]fluoroethoxybenzovesamicol ([^{18}F]FEOBV)

following selective lesion of cholinergic pedunculopontine tegmental neurons in rat. Nucl Med Biol 41: 96–101.

De Carlos JA, Schlaggar BL, O'Leary DD (1995). Development of acetylcholinesterase-positive thalamic and basal forebrain afferents to embryonic rat neocortex. Exp Brain Res 104: 385–401.

Do JP, Xu M, Lee S-H et al. (2016). Cell type-specific long-range connections of basal forebrain circuit. eLife 5: e13214.

Fernandez-Cabello S, Kronbichler M, Van Dijk KRA et al. (2020). Basal forebrain volume reliably predicts the cortical spread of Alzheimer's degeneration. Brain 143: 993–1009.

Freund TF, Gulyás AI (1991). GABAergic interneurons containing calbindin D28K or somatostatin are major targets of GABAergic basal forebrain afferents in the rat neocortex. J Comp Neurol 314: 187–199.

Freund TF, Meskenaite V (1992). Gamma-aminobutyric acid-containing basal forebrain neurons innervate inhibitory interneurons in the neocortex. Proc Natl Acad Sci U S A 89: 738–742.

Fritz H-CJ, Ray N, Dyrba M et al. (2019). The corticotopic organization of the human basal forebrain as revealed by regionally selective functional connectivity profiles. Hum Brain Mapp 40: 868–878.

Gielow MR, Zaborszky L (2017). The input-output relationship of the cholinergic basal forebrain. Cell Rep 18: 1817–1830.

Gritti I, Mainville L, Jones BE (1993). Codistribution of GABA- with acetylcholine-synthesizing neurons in the basal forebrain of the rat. J Comp Neurol 329: 438–457.

Gritti I, Manns ID, Mainville L et al. (2003). Parvalbumin, calbindin, or calretinin in cortically projecting and GABAergic, cholinergic, or glutamatergic basal forebrain neurons of the rat. J Comp Neurol 458: 11–31.

Gritti I, Henny P, Galloni F et al. (2006). Stereological estimates of the basal forebrain cell population in the rat, including neurons containing choline acetyltransferase, glutamic acid decarboxylase or phosphate-activated glutaminase and colocalizing vesicular glutamate transporters. Neuroscience 143: 1051–1064. Elsevier.

Grothe M, Zaborszky L, Atienza M et al. (2010). Reduction of basal forebrain cholinergic system parallels cognitive impairment in patients at high risk of developing Alzheimer's disease. Cereb Cortex 20: 1685–1695.

Grothe M, Heinsen H, Teipel SJ (2012). Atrophy of the cholinergic basal forebrain over the adult age range and in early stages of Alzheimer's disease. Biol Psychiatry 71: 805–813.

Hampel H, Marsel Mesulam M, Claudio Cuello A et al. (2018). The cholinergic system in the pathophysiology and treatment of Alzheimer's disease. Brain 141: 1917–1933.

Hedreen JC, Struble RG, Whitehouse PJ et al. (1984). Topography of the magnocellular basal forebrain system in human brain. J Neuropathol Exp Neurol 43: 1–21.

Henny P, Jones BE (2008). Projections from basal forebrain to prefrontal cortex comprise cholinergic, GABAergic and glutamatergic inputs to pyramidal cells or interneurons. Eur J Neurosci 27: 654–670.

Honey CJ, Sporns O, Cammoun L et al. (2009). Predicting human resting-state functional connectivity from structural connectivity. Proc Natl Acad Sci U S A 106: 2035–2040.

Horti AG, Gao Y, Kuwabara H et al. (2010). Development of radioligands with optimized imaging properties for quantification of nicotinic acetylcholine receptors by positron emission tomography. Life Sci 86: 575–584.

Hur EE, Zaborszky L (2005). Vglut2 afferents to the medial prefrontal and primary somatosensory cortices: a combined retrograde tracing in situ hybridization. J Comp Neurol 483: 351–373.

Jing M, Zhang P, Wang G et al. (2018). A genetically encoded fluorescent acetylcholine indicator for in vitro and in vivo studies. Nat Biotechnol 36: 726–737.

Jones EG, Burton H, Saper CB et al. (1976). Midbrain, diencephalic and cortical relationships of the basal nucleus of Meynert and associated structures in primates. J Comp Neurol 167: 385–419.

Kehagia AA, Barker RA, Robbins TW (2013). Cognitive impairment in Parkinson's disease: the dual syndrome hypothesis. Neurodegener Dis 11: 79–92.

Kikuchi T, Okamura T, Zhang M-R et al. (2013). PET probes for imaging brain acetylcholinesterase. J Label Compd Radiopharm 56: 172–179.

Kilimann I, Grothe M, Heinsen H et al. (2014). Subregional basal forebrain atrophy in Alzheimer's disease: a multicenter study. J Alzheimer's Dis JAD 40: 687–700.

Kim JH, Jung AH, Jeong D et al. (2016). Selectivity of neuromodulatory projections from the basal forebrain and locus ceruleus to primary sensory cortices. J Neurosci 36: 5314–5327.

Kline RL, Zhang S, Farr OM et al. (2016). The effects of methylphenidate on resting-state functional connectivity of the basal nucleus of meynert, locus coeruleus, and ventral tegmental area in healthy adults. Front Human Neurosci Front 10: 149.

Koh S, Loy R (1989). Localization and development of nerve growth factor-sensitive rat basal forebrain neurons and their afferent projections to hippocampus and neocortex. J Neurosci 9: 2999–3018.

Kondo H, Zaborszky L (2016). Topographic organization of the basal forebrain projections to the perirhinal, postrhinal, and entorhinal cortex in rats. J Comp Neurol 524: 2503–2515.

Kuchibhotla KV, Gill JV, Lindsay GW et al. (2017). Parallel processing by cortical inhibition enables context-dependent behavior. Nat Neurosci 20: 62–71.

Laszlovszky T, Schlingloff D, Hegedüs P et al. (2020). Distinct synchronization, cortical coupling and behavioral function of two basal forebrain cholinergic neuron types. Nat Neurosci 23: 992–1003.

Letzkus JJ, Wolff SBE, Meyer EMM et al. (2011). A disinhibitory microcircuit for associative fear learning in the auditory cortex. Nature 480: 331–335.

Li C-SR, Ide JS, Zhang S et al. (2014). Resting state functional connectivity of the basal nucleus of Meynert in humans: in comparison to the ventral striatum and the effects of age. Neuroimage 97: 321–332.

Li X, Yu B, Sun Q et al. (2018). Generation of a whole-brain atlas for the cholinergic system and mesoscopic projectome analysis of basal forebrain cholinergic neurons. Proc Natl Acad Sci U S A 115: 415–420.

Lin SC, Brown RE, Hussain Shuler MG et al. (2015). Optogenetic dissection of the basal forebrain neuromodulatory control of cortical activation, plasticity, and cognition. J Neurosci 35: 13896–13903.

Liu Q, Zhu Z, Teipel SJ et al. (2017). White matter damage in the cholinergic system contributes to cognitive impairment in subcortical vascular cognitive impairment, no dementia. Front Aging Neurosci 9: 47.

López-Hernández GY, Ananth M, Jiang L et al. (2017). Electrophysiological properties of basal forebrain cholinergic neurons identified by genetic and optogenetic tagging. J Neurochem 142: 103–110.

Malmquist J, Varnäs K, Svedberg M et al. (2018). Discovery of a novel muscarinic receptor PET radioligand with rapid kinetics in the monkey brain. ACS Chem Nerosci 9: 224–229.

Markello RD, Spreng RN, Luh W-M et al. (2018). Segregation of the human basal forebrain using resting state functional MRI. Neuroimage 173: 287–297.

Merker B (1983). Silver staining of cell bodies by means of physical development. J Neurosci Methods 9: 235–241.

Mesulam MM, Geula C (1988). Nucleus basalis (Ch4) and cortical cholinergic innervation in the human brain: observations based on the distribution of acetylcholinesterase and choline acetyltransferase. J Comp Neurol 275: 216–240.

Mesulam M-M, Van Hoesen GW (1976). Acetylcholinesterase-rich projections from the basal forebrain of the rhesus monkey to neocortex. Brain Res 109: 152–157.

Mesulam MM, Mufson EJ, Levey AI et al. (1983a). Cholinergic innervation of cortex by the basal forebrain: cytochemistry and cortical connections of the septal area, diagonal band nuclei, nucleus basalis (substantia innominata), and hypothalamus in the rhesus monkey. J Comp Neurol 214: 170–197.

Mesulam MM, Mufson EJ, Wainer BH et al. (1983b). Central cholinergic pathways in the rat: an overview based on an alternative nomenclature (Ch1-Ch6). Neuroscience 10: 1185–1201.

Mueller SG, Weiner MW, Thal LJ et al. (2005). Ways toward an early diagnosis in Alzheimer's disease: the Alzheimer's Disease Neuroimaging Initiative (ADNI). Alzheimers Dement 1: 55–66.

Mufson EJ, Bothwell M, Hersh LB et al. (1989). Nerve growth factor receptor immunoreactive profiles in the normal, aged human basal forebrain: colocalization with cholinergic neurons. J Comp Neurol 285: 196–217.

Mulholland GK, Wieland DM, Kilbourn MR et al. (1998). [18F] fluoroethoxy-benzovesamicol, a PET radiotracer for the vesicular acetylcholine transporter and cholinergic synapses. Synapse 30: 263–274.

Muñoz W, Rudy B (2014). Spatiotemporal specificity in cholinergic control of neocortical function. Curr Opin Neurobiol 26: 149–160.

Nejad-Davarani S, Koeppe RA, Albin RL et al. (2019). Quantification of brain cholinergic denervation in dementia with Lewy bodies using PET imaging with [18 F]-FEOBV. Mol Psychiatry 24: 322–327.

Nemy M, Cedres N, Grothe MJ et al. (2020). Cholinergic white matter pathways make a stronger contribution to attention and memory in normal aging than cerebrovascular health and nucleus basalis of Meynert. Neuroimage 211: 116607.

Obermayer J, Verhoog MB, Luchicchi A et al. (2017). Cholinergic modulation of cortical microcircuits is layer-specific: evidence from rodent, monkey and human brain. Front Neural Circuits 11: 100.

Parent M, Bedard MA, Aliaga A et al. (2012). PET imaging of cholinergic deficits in rats using [18F]fluoroethoxybenzovesamicol ([18F]FEOBV). Neuroimage 62: 555–561.

Pearson RC, Gatter KC, Powell TP (1983). The cortical relationships of certain basal ganglia and the cholinergic basal forebrain nuclei. Brain Res 261: 327–330.

Pereira JB, Hall S, Jalakas M et al. (2020). Longitudinal degeneration of the basal forebrain predicts subsequent dementia in Parkinson's disease. Neurobiol Dis 139: 104831.

Picciotto MR, Higley MJ, Mineur YS (2012). Acetylcholine as a neuromodulator: cholinergic signaling shapes nervous system function and behavior. Neuron 76: 116–129.

Pinto L, Goard MJ, Estandian D et al. (2013). Fast modulation of visual perception by basal forebrain cholinergic neurons. Nat Neurosci 16: 1857–1863.

Pombero A, Bueno C, Saglietti L et al. (2011). Pallial origin of basal forebrain cholinergic neurons in the nucleus basalis of Meynert and horizontal limb of the diagonal band nucleus. Development 138: 4315–4326.

Ray NJ, Bradburn S, Murgatroyd C et al. (2018). In vivo cholinergic basal forebrain atrophy predicts cognitive decline in de novo Parkinson's disease. Brain 141: 165–176.

Richter N, Beckers N, Onur OA et al. (2018). Effect of cholinergic treatment depends on cholinergic integrity in early Alzheimer's disease. Brain 141: 903–915.

Richter N, Nellessen N, Dronse J et al. (2019). Spatial distributions of cholinergic impairment and neuronal hypometabolism differ in MCI due to AD. NeuroImage Clin 24: 101978.

Saper CB, Chelimsky TC (1984). A cytoarchitectonic and histochemical study of nucleus basalis and associated cell groups in the normal human brain. Neuroscience 13: 1023–1037.

Sarter M, Lustig C (2020). Forebrain cholinergic signaling: wired and phasic, not tonic, and causing behavior. J Neurosci 40: 712–719.

Sarter M, Parikh V, Howe WM (2009). Phasic acetylcholine release and the volume transmission hypothesis: time to move on. Nat Rev Neurosci 10: 383–390.

Saunders A, Granger AJ, Sabatini BL (2015). Corelease of acetylcholine and GABA from cholinergic forebrain neurons. eLife 4: e06412.

Scheef L, Grothe MJ, Koppara A et al. (2019). Subregional volume reduction of the cholinergic forebrain in subjective cognitive decline (SCD). NeuroImage Clin 21: 101612.

Schmitz TW, Duncan J (2018). Normalization and the cholinergic microcircuit: a unified basis for attention. Trends Cogn Sci 22: 422–437.

Schmitz TW, Spreng RN (2016). Basal forebrain degeneration precedes and predicts the cortical spread of Alzheimer's pathology. Nat Commun 7: 13249.

Schmitz TW, Mur M, Aghourian M et al. (2018). Longitudinal Alzheimer's degeneration reflects the spatial topography of cholinergic basal forebrain projections. Cell Rep 24: 38–46.

Schmitz TW, Soreq H, Poirier J et al. (2020). Longitudinal basal forebrain degeneration interacts with TREM2/C3 biomarkers of inflammation in pre-symptomatic Alzheimer's disease. J Neurosci 40: 1931–1942.

Schrag A, Siddiqui UF, Anastasiou Z et al. (2017). Clinical variables and biomarkers in prediction of cognitive impairment in patients with newly diagnosed Parkinson's disease: a cohort study. Lancet Neurol 16: 66–75.

Schulz J, Pagano G, Fernandez Bonfante JA et al. (2018). Nucleus basalis of Meynert degeneration precedes and predicts cognitive impairment in Parkinson's disease. Brain 141: 1501–1516.

Selden NR, Gitelman DR, Mesulam M-M (1998). Trajectories of corticopetal cholinergic pathways within the cerebral hemispheres of the human brain. Neuro-Image 7: S26.

Semba K, Fibiger HC (1988). Time of origin of cholinergic neurons in the rat basal forebrain. J Comp Neurol 269: 87–95.

Skudlarski P, Jagannathan K, Calhoun VD et al. (2008). Measuring brain connectivity: diffusion tensor imaging validates resting state temporal correlations. Neuroimage 43: 554–561.

Spillantini MG, Schmidt ML, Lee VM et al. (1997). Alpha-synuclein in Lewy bodies. Nature 388: 839–840.

Tang Y, Mishkin M, Aigner TG (1997). Effects of muscarinic blockade in perirhinal cortex during visual recognition. Proc Natl Acad Sci U S A 94: 12667–12669.

Teipel SJ, Flatz WH, Heinsen H et al. (2005). Measurement of basal forebrain atrophy in Alzheimer's disease using MRI. Brain 128: 2626–2644.

Teipel SJ, Meindl T, Grinberg L et al. (2011). The cholinergic system in mild cognitive impairment and Alzheimer's disease: an in vivo MRI and DTI study. Hum Brain Mapp 32: 1349–1362.

Teipel SJ, Wohlert A, Metzger C et al. (2017). Multicenter stability of resting state fMRI in the detection of Alzheimer's disease and amnestic MCI. NeuroImage Clin 14: 183–194.

Tu Z, Zhang X, Jin H et al. (2015). Synthesis and biological characterization of a promising F-18 PET tracer for vesicular acetylcholine transporter. Bioorg Med Chem 23: 4699–4709.

Unal CT, Pare D, Zaborszky L (2015). Impact of basal forebrain cholinergic inputs on basolateral amygdala neurons. J Neurosci 35: 853–863.

Verhoog MB, Obermayer J, Kortleven CA et al. (2016). Layer-specific cholinergic control of human and mouse cortical synaptic plasticity. Nat Commun 7: 12826.

Williams-Gray CH, Evans JR, Goris A et al. (2009). The distinct cognitive syndromes of Parkinson's disease: 5 year follow-up of the CamPaIGN cohort. Brain 132: 2958–2969.

Williams-Gray CH, Mason SL, Evans JR et al. (2013). The CamPaIGN study of Parkinson's disease: 10-year outlook in an incident population-based cohort. J Neurol Neurosurg Psychiatry 84: 1258–1264.

Winters BD, Forwood SE, Cowell RA et al. (2004). Double dissociation between the effects of peri-postrhinal cortex and hippocampal lesions on tests of object recognition and spatial memory: heterogeneity of function within the temporal lobe. J Neurosci 24: 5901–5908.

Woolf NJ (1991). Cholinergic systems in mammalian brain and spinal cord. Prog Neurobiol 37: 475–524.

Wu H, Williams J, Nathans J (2014). Complete morphologies of basal forebrain cholinergic neurons in the mouse. eLife 3: e02444.

Xu M, Chung S, Zhang S et al. (2015). Basal forebrain circuit for sleep-wake control. Nat Neurosci 18: 1641–1647.

Yuan R, Biswal BB, Zaborszky L (2019). Functional subdivisions of magnocellular cell groups in human basal forebrain: test–retest resting-state study at ultra-high field, and meta-analysis. Cerebral Cortex 29: 2844–2858.

Zaborszky L, Carlsen J, Brashear HR et al. (1986). Cholinergic and GABAergic afferents to the olfactory bulb in the rat with special emphasis on the projection neurons in the nucleus of the horizontal limb of the diagonal band. J Comp Neurol 243: 488–509.

Zaborszky L, Hoemke L, Mohlberg H et al. (2008). Stereotaxic probabilistic maps of the magnocellular cell groups in human basal forebrain. Neuroimage 42: 1127–1141.

Záborszky L, Amunts K, Palomero-Gallagher N et al. (2015). Basal forebrain anatomical systems in MRI space. In: Brain mapping: an encyclopedic reference, Elsevier Inc. 395–409.

Zaborszky L, Csordas A, Mosca K et al. (2015). Neurons in the basal forebrain project to the cortex in a complex topographic organization that reflects corticocortical connectivity patterns: an experimental study based on retrograde tracing and 3D reconstruction. Cereb Cortex 25: 118–137.

Zaborszky L, Gombkoto P, Varsanyi P et al. (2018). Specific basal forebrain-cortical cholinergic circuits coordinate cognitive operations. J Neurosci 38: 9446–9458.

Zhang S, Hu S, Fucito LM et al. (2017). Resting-state functional connectivity of the basal nucleus of Meynert in cigarette smokers: dependence level and gender differences. Nicotine Tob Res 19: 452–459.